Int. J. Heat Mass Transfer. Vol. 28, No. 3, pp. 663–673, 1985
Printed in Great Britain

0017–9310/85 $3.00 + 0.00

Temperature distribution within the left ventricular wall of the heart

E. BARTA, R. BEYAR and S. SIDEMAN

Departments of Biomedical and Chemical Engineering, The Julius Silver Institute of Biomedical Engineering, Technion–Israel Institute of Technology, Haifa 32000, Israel

(*Received* 26 *July* 1984)

Abstract—The instantaneous local temperature T throughout the left ventricle (LV) wall is obtained by solving the energy balance equation, accounting for the instantaneous spatial heat generation within muscle wall. The distributed oxygen demand as well as time dependent local coronary perfusion, which are based on a previously described mechanical model of the LV, are used as input parameters to the heat equation. Approximations of the local time averaged and the time-dependent temperatures are computed for two types of experimental boundary conditions simulating (a) closed chest heart (given epicardial T) and (b) an open chest heart (exposed to air with free convection). The effects of the heart rate and the local blood perfusion rate on T are investigated. The local temperature is found to be practically unchanged throughout a cycle, with changes which are typically smaller than 0.005°C during a cycle. However, the temperature varies with the location within the myocardium and attains its maximum value at the mid-layers. For a closed chest heart, an approximation of the instantaneous temperature based on the 'average' solution is found. In case of an open chest heart, it is shown how T in the epicardium can define the temperature distribution throughout the entire muscle wall. The calculated results are found to be in fair agreement with experimental studies in dogs.

1. INTRODUCTION

APART FROM the inherent basic curiosity to elucidate the secrets of nature, the search for a comprehensive solution of the spatial and temporal temperature distribution within the myocardium, the muscle that makes up the wall of the heart, may lead to a better and more complete understanding of the complex interactions between the myocardial mechanics, metabolism and the blood perfusion that continuously nourishes this muscle in a cyclic rhythm. Furthermore, since slight changes in the temperature, may yield significant changes in the depolarization patterns [1], throughout the muscle, a better understanding of the temperature distribution in the cardiac wall may help in understanding the highly complex phenomenon of a different electrical activity in different regions of the myocardium.

Obviously, the solution of this complicated problem depends upon the availability of well defined quantitative theoretical and/or experimental data about the local instantaneous blood perfusion and oxygen consumption within the myocardium. Concentrating on the left ventricle (LV) of the heart, numerous models have been proposed to describe the mechanics of contraction [2–4]. Concurrently, metabolic models [5–7] and coronary flow models [8, 9] were also studied. However, these models were not, until recently, appropriately combined to account for the distributed nature of the transmural energy balance. A normal pattern which involves higher endocardial values of perfusion and oxygen consumption are well documented by Feigl [10].

Hernandez *et al.* [11] solved the inverse problem in heat generation and conduction. The blood perfusion and oxygen consumption, assumed evenly distributed and constant with time, were computed based on the assumption that the temperature distribution is given from measurements. Ten Velden *et al.* [12] used an analytical method to calculate the local temperature in the myocardium by neglecting the time dependent variation in the perfusion, oxygen consumption and temperature. Smaill *et al.* [13] used constant and steady-state blood perfusion and oxygen consumption values for solving the heat balance equation in the three dimensional LV wall by a finite element method. To the best of our knowledge, the above models are the only ones that provide a method to calculate the temperature distribution throughout the myocardium, and as such are limited by their inherent steady-state assumptions and the omission of the distributed nature of the blood perfusion and oxygen consumption.

Several experimental measurements of the temperature in the myocardium were reported; Ten Velden *et al.* [12] measured the local *in vivo* temperature in the canine LV myocardium. Hernandez *et al.* [11] measured the temperature in three layers of the canine myocardium. Reynolds *et al.* [1] measured the temperature in closed chest canine myocardium as well as the temperature in the human right and left ventricles. This was accomplished by pulling a fine thermocouple through a previously punctured pathway through the LV, right ventricle and lungs. It is interesting that the latter, but earlier, experiments indicate that the temperature in the epicardium is higher than that in the endocardium, in contradiction to the more recent data. This also contradicts the recent observations by Eberhart [14] which indicate higher

NOMENCLATURE

A^n	the matrix in the matrix form of the numerical scheme for the heat equation
$\mathbf{b}^n$	the constants vector in the matrix form of the numerical scheme for the heat equation
c	heat capacity constant of the myocardium [J g^{-1} °C^{-1}]
c_b	heat capacity constant of the blood [J g^{-1} °C^{-1}]
$c_2(r,t)$, $c_2(r)$	coefficients in the heat balance equation [cm^{-2}, °C cm^{-2}]
h	free heat convection constant [W m^{-2} °C^{-1}]
k	heat conduction constant [W cm^{-1} °C^{-1}]
$\dot{m}(r,t)$	blood perfusion in the left ventricular wall [ml s^{-1} g^{-1}]
$m[r_i, r_{i+1}]$	the average blood volume that flows between r_i and r_{i+1} [cm^3]
$\dot{q}_m(r)$	heat due to metabolic energy [J cm^{-3} s^{-1}]
r	the radial distance measured from the centre of the ventricle to a point at the wall [cm]
r_j^n	the distance of the jth point in the radial net from the centre for $t = n0.01$ s [cm]
R_1, R_2	the radial distance of the endocardium and the epicardium respectively from the centre of the ventricle [cm]
t	time [s]
$T(r,t)$	instantaneous local temperature in the myocardium [°C]
T_A	epicardial temperature [°C]
T_b	blood temperature [°C]
T_∞	air temperature [°C]
$u(r,t)$	instantaneous local difference between the temperature of the myocardium and the blood [°C]
$\bar{u}(r)$	'average' local temperature in the myocardium [°C]
$\tilde{u}(0,r)$	approximate local temperature in the myocardium [°C]
u_δ^n	the numerical value of $u(r = r_j^n, t = n0.01$ s) [°C]
$V[r_i, r_{i+1}]$	the average volume of the muscle layer that extends from r_i to r_{i+1} [cm^3]
α	the thermal diffusivity [cm^2 s^{-1}]
$\lambda_i(A^n)$	the eigenvalues of the matrix A^n
Δr_j^n	the radial grid spacing between the points r_{j-1}^n and r_j^n in the numerical scheme [cm]
Δt	the time grid spacing in the numerical scheme [s]
ΔT_{VA}	veno-arterioral temperature difference [°C]
ρ	the myocardial density [g cm^{-3}]
ρ_b	the blood density [g cm^{-3}]
τ	the duration of one heart cycle [s].

endocardial than epicardial temperatures. Related measurements of the veno-arterioral temperature difference were reported by Neill *et al.* [15], and these are used below as another indication of the validity of our results.

In this paper we use the recently integrated LV model of Beyar and Sideman [16–18] which combined the mechanical parameters of contraction, based on a spheroidal nested shell geometry, with the time-dependent distributed coronary perfusion (Fig. 1) and the time-averaged distribution of oxygen consumption (Fig. 2). The energy balance includes the principal mechanisms which are involved in heat transfer and heat generation, assuming aerobic metabolism. An axial symmetry assumption simplifies the formulation of the problem and a numerical solution is obtained for closed and open chest hearts. The so-called average local temperature and the instantaneous local temperature are computed using the shooting method [19] and explicit difference scheme, respectively.

2. THE MATHEMATICAL FORMULATION

2.1. *The heat balance equation*

The mechanisms that control heat generation and transfer in the LV muscle are the generation of heat by chemical processes involved in basic metabolism and by the mechanical activity of the heart, the convection of heat by the perfusion of blood and conduction of heat through the LV wall.

The temperature distribution is computed by solving the heat balance equation which is formulated for the transverse section through the equator of a spheroid (Fig. 3), consistent with the solutions obtained for the oxygen consumption [17] and coronary perfusion [16].

It is assumed that the thermal diffusivity of the muscle $\alpha = k/\rho c$ is uniform through the muscle. In addition, it is assumed that the epicardium and the endocardium have uniform temperatures. This defines the symmetry of the problem, and thus the temperature gradient has

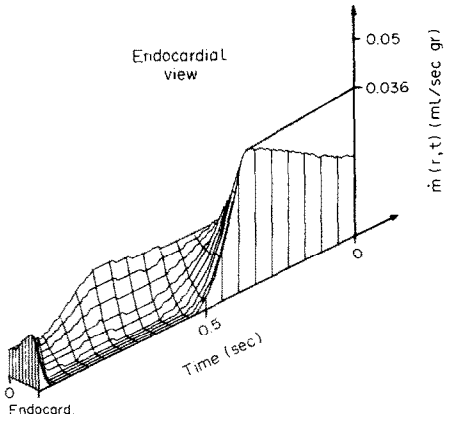

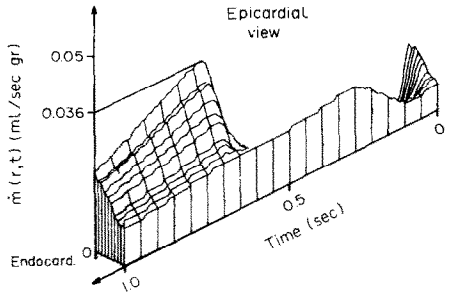

FIG. 1. Distribution of time-dependent coronary perfusion in human during one cardiac cycle. Typical rest conditions.

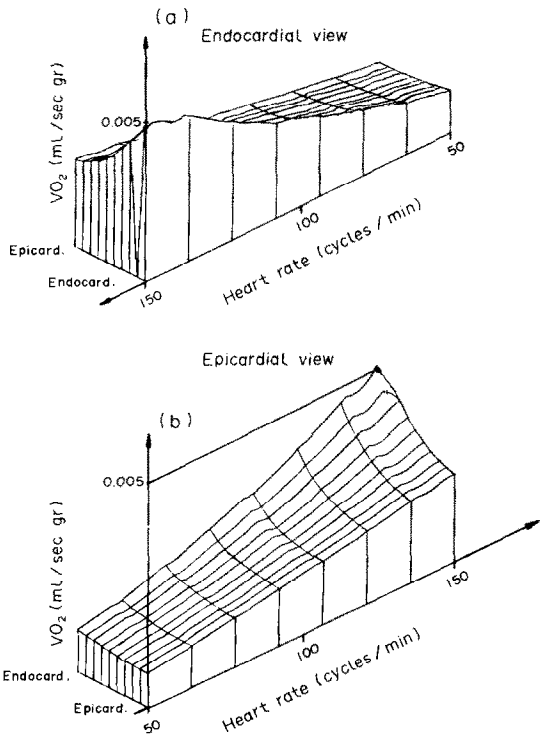

FIG. 2. Distribution of time-averaged oxygen consumption as a function of the heart rate.

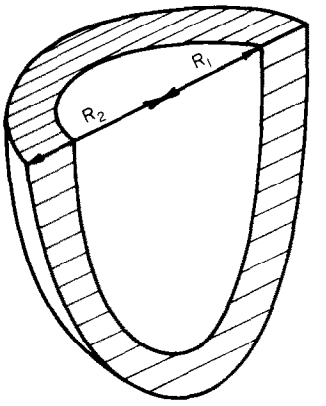

FIG. 3. Spheroidal representation of the LV.

only a radial component. Thus, the heat balance in the range $R_1 \leqslant r \leqslant R_2$, $0 \leqslant T \leqslant \tau$ is given by

$$\frac{1}{\alpha}\frac{\partial u}{\partial t} = \frac{\partial^2 u}{\partial r^2} + \frac{1}{r}\frac{\partial u}{\partial r} + c_1(r,t)u + c_2(r), \tag{1}$$

where

$$u = T - T_b, \tag{2}$$

$$c_1(r,t) = -\frac{\dot{m}(r,t)\cdot\rho\cdot\rho_b\cdot c_b}{k}, \tag{3}$$

$$c_2(r) = \frac{\dot{q}_m(r)}{k}. \tag{4}$$

τ is the duration of one heart cycle and r is the radial distance measured from the centre to a point at the wall between R_1 and R_2, the endocardium and the epicardium, respectively. Subscript b denotes the blood while variables with no subscript refer to the muscle. $\dot{m}(r,t)$ is the blood perfusion rate per unit mass of muscle, $\dot{q}_m(r)$ is the total metabolic heat production rate per unit muscle mass; $\dot{q}_m(r)$ is evaluated by relating to 75% of the calculated local oxygen consumption. This is consistent with the fact that only 20–30% of the metabolic energy is used for the mechanical pumping work [20] and the rest is converted to heat. The energy equivalent of the oxygen consumption is taken here as 4.7 cal cm^{-3} O_2 corresponding to a respiratory quotient (RQ), defined as the molar ratio of CO_2 produced per O_2 metabolized, of 0.7, [21]. Thus,

$$\dot{q}_m(r) = (4.7 \times 0.75)\cdot\rho\cdot V_{O_2} = 3.525\cdot\rho\cdot V_{O_2} \tag{5}$$

where V_{O_2} is the oxygen demand rate per unit mass of muscle. Other values might be used as well (according to the metabolic pathways which are active) as given by Neill *et al.* [21]

2.2. *The boundary conditions*

The muscle temperature at the endocardium is assumed equal to the bulk temperature of blood, T_b, in the LV cavity. This is reasonable in view of the conditions of direct contact of the wall with a relatively

large amount of blood [13]. Thus,

$$u(t, R_1) = 0 \quad 0 \leqslant t \leqslant \tau. \tag{6}$$

Depending on the experimental set up, two different boundary conditions can be used for the epicardium. For the closed chest case we use an *a priori* known value for the temperature at the epicardium which is taken to be approximately constant with time [13]. Thus,

$$u(t, R_2) = u_A \quad 0 \leqslant t \leqslant \tau. \tag{7}$$

When the heart is exposed to air (open chest), there is a free convection on the epicardium, expressed by

$$-k\frac{\partial u}{\partial r}(t, R_2) = h[u(t, R_2) - u_\infty] \quad 0 \leqslant t \leqslant \tau \tag{8}$$

where $u_\infty = T - T_\infty$; T_∞ is the air temperature and h is the free convection heat transfer coefficient (assumed constant). Thus, different values are obtained for the epicardial temperature for different flow rates and different oxygen consumption rates.

Finally, the periodicity boundary condition is given by

$$u(0, r) = u(\tau, r) \quad R_1 \leqslant r \leqslant R_2. \tag{9}$$

3. APPROXIMATE TIME-INDEPENDENT SOLUTIONS

An approximate solution for the temperature distribution within the wall can be obtained by formulating equation (1) as a time-independent problem. Obviously, this approach can be used to yield the initial temperature distribution required to solve equation (1). A successful estimation of the initial conditions will shorten the convergence time and save computer time.

A reasonable approximation of the initial temperature distribution is obtained by integrating equation (1) over the whole cycle yielding

$$0 = \frac{1}{\tau}\left[\int_0^\tau \frac{\partial^2 u}{\partial r^2}\,dt + \int_0^\tau \frac{1}{r}\frac{\partial u}{\partial r}\,dt + \int_0^\tau c_1 \cdot u\,dt\right] + c_2(r). \tag{10}$$

Using the assumptions that $u(t, r) \simeq \bar{u}(r)$, i.e. the temperature does not change with time;

$$\frac{\partial u(t, r)}{\partial r} \simeq \frac{\partial \bar{u}(r)}{\partial r}$$

and

$$\frac{\partial^2 u(t, r)}{\partial r^2} \simeq \frac{\partial^2 \bar{u}(r)}{\partial r^2},$$

i.e. the derivatives of the temperature with respect to location are independent of time, yields

$$0 \simeq \frac{d^2\bar{u}}{dr^2} + \frac{d\bar{u}}{dr}\cdot\left(\frac{1}{\tau}\int_0^\tau \frac{1}{r}\,dt\right) + \bar{u}\left(\frac{1}{\tau}\int_0^\tau c_1\,dt\right) + c_2. \tag{11}$$

The shooting method, described by Keller [19] (IMSL Library) is used in solving equation (11) for the boundary conditions given by equations (6)–(8) yielding the 'average' time independent temperature profile within the wall.

The more 'natural' procedure for the approximation of the initial temperature based on the omission of the left side of equation (1) and using only the initial values of the perfusion and LV geometry, gives rather poor results. The heat balance equation in this case is

$$0 = \frac{d^2u}{dr^2} + \frac{1}{r}\frac{du}{dr} + c_1(r)u + c_2(r) \tag{12}$$

and boundary conditions, equations (6)–(8) remain unchanged. The solution of the temperature distribution in this time-independent formulation (12) can be found by using the same shooting method.

Note that different temperature distributions will evolve when this approximation is utilized with coronary flow data which corresponds to different times during the cycle. This indicates that equation (12) is an illegitimate approximation. The reason for this is quite clear: Even if the temperature at a point changes very slowly with time (so that $\partial u/\partial t$ is very small), the thermal diffusivity α, which is very small for the muscle tissue gives the whole left term a non-negligible significance.

4. THE NUMERICAL SOLUTION

The physical constants used in the model are summarized in Table 1. The relevant hemodynamic parameters concerning the heart function are chosen to correspond to a normal heart working under resting conditions and are summarized in Table 2. The heart rate, HR, ranges from 60 to 120 cpm.

The numerical network is the same as before [16–18], i.e. a time step of 0.01 s and 10 equal thickness layers of the wall $(R_2 - R_1)$ taken at the reference, unstressed configuration of the LV. Thus, a net of 11 points, nonuniformly distributed, characterizes each step in time.

Starting from an initial approximate value $\bar{u}$, given by the solution of equation (11), an explicit numerical scheme, using forward difference for the time derivative and central differences for the radial derivatives, is applied,

$$\frac{1}{\alpha}\cdot\frac{u_j^{n+1} - u_j^n}{\Delta t} = \frac{\Delta r_{j-1}^n u_{j+1}^n + \Delta r_j^n u_{j-1}^n - (\Delta r_j^n + \Delta r_{j-1}^n)u_j^n}{\frac{1}{2}\Delta r_{j-1}^n \Delta r_j^n (\Delta r_j^n + \Delta r_{j-1}^n)} + \frac{1}{r_j^n}\cdot\frac{u_{j+1}^n - u_{j-1}^n}{\Delta r_j^n + \Delta r_{j-1}^n} + c_1(r_j^n) + c_2(r_j^n) \tag{13}$$

$$\Delta t = 0.01\text{ s}, \quad n = 1, \ldots, (N-1), \quad N = 100\tau$$

$$r_j^n = r_{j-1}^n + \Delta r_{j-1}^n$$

Table 1. Constants used in the model, see [11]

Parameter	Value
k	0.0058 W cm^{-1} °C^{-1}
ρ_b	1.02 g cm^{-3}
ρ	1.07 g cm^{-3}
c_b	3.725 J g^{-1} °C^{-1}
c	3.725 J g^{-1} °C^{-1}

where r_j^n is the distance of the jth point from the centre in the radial net for $t = n \cdot 0.01$ s and u_j^n is the numerical value of u at point r_j^n. All the computations were run on an IBM 380.

4.1. *Given epicardial temperature (closed chest heart)*

Given measurements of epicardial T in closed chest hearts are available and can be used in the solution of the problem. In this case equation (11) is applied for $j = 2,\ldots,10$ and the temperature at both ends ($j = 1$, 11) is known. Following Ten Velden *et al.* [12] we assume that the epicardial temperature is lower than the endocardial temperature by 0.25°C, i.e.

$$u_{11}^n = -0.25°C \quad n = 1,\ldots,N. \tag{14}$$

The consistency of the numerical scheme is quite clear since the local truncation error, TE, of equation (13) is

$$TE = 0\{\max(\Delta t, |\Delta r_j^n - \Delta r_{j-1}^n|\} = 0(0.01).$$

The stability is verified (Appendix A), thus proving the convergence, i.e. stability and consistency, of equation (13) to the solution of equation (1). The solution is found by computing equation (13) iteratively until the periodicity condition is satisfied within a maximal error of 5×10^{-6} °C.

4.2. *Free convection at the epicardium (open chest case)*

Considering the difference between the temperature of the air and the temperature of the wall in the open chest heart makes it reasonable to analyze this case with a free convection boundary condition at the epicardium, equation (8).

The numerical solution u_j^n for $j = 2,\ldots,10$ is computed by equation (13). u_{11}^n is found by adding an artificial point, r_{12}^n, to the net and solving simultaneously the two equations

$$\frac{1}{\alpha}\frac{u_{11}^{n+1} - u_{11}^n}{\Delta t} = \frac{u_{12}^n + u_{10}^n - 2u_{11}^n}{(2\Delta r_{10}^n)^2} - \frac{h}{r_{11}^n k} \times (u_{11}^n - u_\infty) + c_1(r_{11}^n)u_{11}^n + c_2(r_{11}^n) \tag{15}$$

$$-k\left(\frac{u_{12}^n - u_{10}^n}{2\Delta r_{10}^n}\right) = h(u_{11}^n - u_\infty) \quad n = 1,\ldots,N-1. \tag{16}$$

Obviously, the scheme is consistent. As a matter of fact, the computations indicate that the scheme does not diverge. The proof that the solution does not converge to a wrong value, is given in Appendix A. The computations are terminated when the accuracy criterion is met.

5. RESULTS

5.1. *General*

Some of the calculated results are presented in Figs. 4–11. Note that the temperature profiles in these figures represent the temperature distribution when $t = 0$. However, since the temperature at a point is practically time-independent (within a slight deviation) these curves represent the temperature at any time. (The maximum variation with time of the temperature for HR = 90 cpm is 0.0024°C for a closed chest heart with a given epicardial temperature and 0.0047°C for an opened chest heart with the free convection case.) This insignificant time variation of the local temperatures explains the relatively small difference between the approximate 'average' temperature and the complete time-dependent solution in Figs. 4 and 8. The slight differences between the curves are mainly due to the assumptions we made in computing $\bar{u}$.

For the constant temperature boundary conditions (closed chest case) a more accurate time-independent temperature profile is obtained by applying a minimum

Table 2. Hemodynamic parameters at rest for human and dog data [16–18]

	Human (h)			Dog (h)
Parameter	60	90	120	90
Initial short semiaxis (cm)	2.3	2.3	2.3	1.91
Initial (end diastolic) volume (ml)	101.9	101.9	101.9	52.0
End systolic volume (ml)	33.7	28.0	24.0	21.0
Stroke volume (ml)	68	74	78	31
Cardiac output (ml min^{-1})	4096	6654	9349	2844
Ejection fraction (%)	67	72	76	60
Arterial pressure (mmHg)	131/85	128/85	129/85	126/85
Average oxygen consumption (ml s^{-1} g^{-1})	0.0013	0.0019	0.0026	0.0017
Average coronary perfusion (ml s^{-1} g^{-1})	0.011	0.013	0.018	0.011

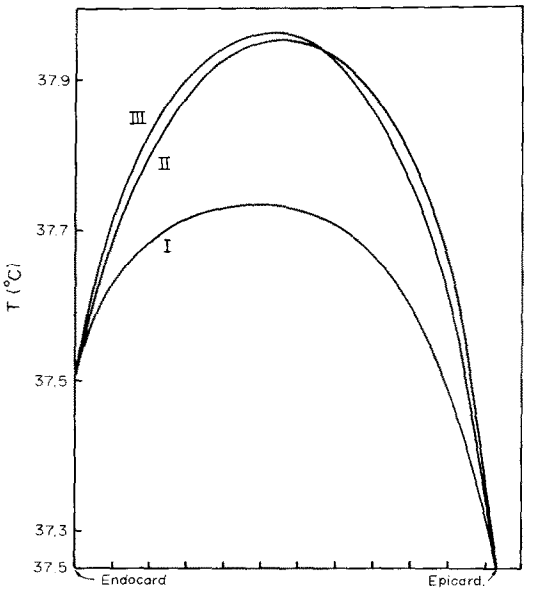

FIG. 4. The myocardial temperature distribution for $T_b = 37.5°C$, $U_A = -0.25°C$. HR = 120 cpm. I, Time-independent solution using data of $t = 0$; II, 'average' solution, $\bar{u}$; III, complete time-dependent solution at $t = 0$.

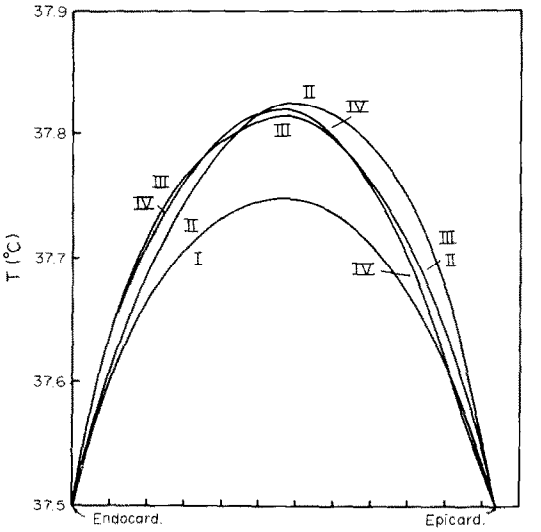

FIG. 5. The myocardial temperature distribution for $T_b = 37.5°C$, $U_A = 0°C$, HR = 60 cpm. I, Time-independent solution using data of $t = 0$; II, 'average' solution, $\bar{u}$; III, complete time-dependent solution at $t = 0$; IV, $\tilde{u}$ the temperature according to equation (17).

least-square criterion, to the calculated values of the time-dependent and time-independent solutions. Thus

$$\tilde{u}(0,r) = \begin{cases} 1.19\bar{u}(r) & r_1^n \leqslant r \leqslant r_2^n \\ 1.10\bar{u}(r) & r_2^n \leqslant r \leqslant r_3^n \\ 1.04\bar{u}(r) & r_3^n \leqslant r \leqslant r_4^n \\ 1.01\bar{u}(r) & r_4^n \leqslant r \leqslant r_5^n \\ 0.98\bar{u}(r) & r_5^n \leqslant r \leqslant r_6^n \\ 0.93\bar{u}(r) & r_6^n \leqslant r \leqslant r_7^n \\ 0.88\bar{u}(r) & r_7^n \leqslant r \leqslant r_8^n \\ 0.79\bar{u}(r) & r_8^n \leqslant r \leqslant r_9^n \\ 0.57u(r) & r_9^n \leqslant r \leqslant r_{10}^n. \end{cases} \quad (17)$$

The accuracy of the approximation, $\bar{u}$, for a case of $u(t, R_2) = 0°C$ is shown in Fig. 5, indicating that although equation (17) is based only on computations with equation (14) as a boundary condition, it might be helpful when other constant temperature boundary conditions are applied.

5.2. *Given epicardial temperature*

The dependence of the temperature distribution on the heart rate, HR, and the blood perfusion rate $\dot{m}(r, t)$, are shown in Figs. 6 and 7, respectively. As expected, increasing HR and/or decreasing $\dot{m}(r, t)$ increases the temperature throughout the wall. As seen in Figs. 4–7, the maximum temperature is attained approximately at the middle of the wall and the temperature gradients increase toward the boundaries.

5.3. *Free convection solution*

Free convection of air is characterized by heat transfer coefficients (HTC) from 5 to 25 W m^{-2} °C^{-1}, [22], and h values ranging from 12.5 to 27 W m^{-2} °C^{-1} were used here. The HTC is not *a priori* known but, conceivably, one can measure the epicardial temperature and then determine the corresponding value of h. Figure 8 compares the solutions obtained by the time-dependent and approximate time-independent procedures. Again, the utility of the average solution is evident.

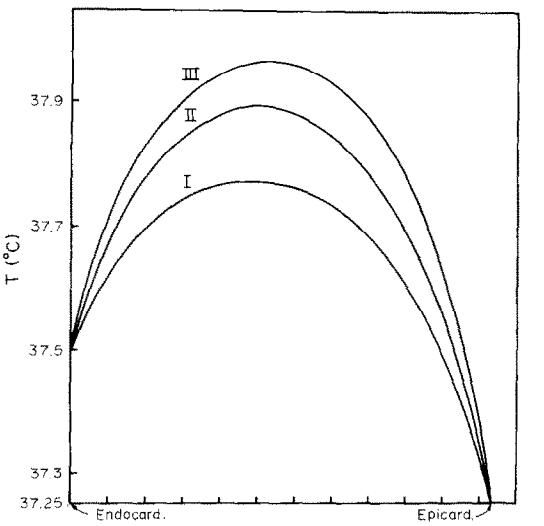

FIG. 6. The myocardial temperature distribution at $t = 0$, $T_b = 37.5°C$, $U_A = -0.25°C$. I, HR = 60 cpm; II, HR = 90 cpm; III, HR = 120 cpm.

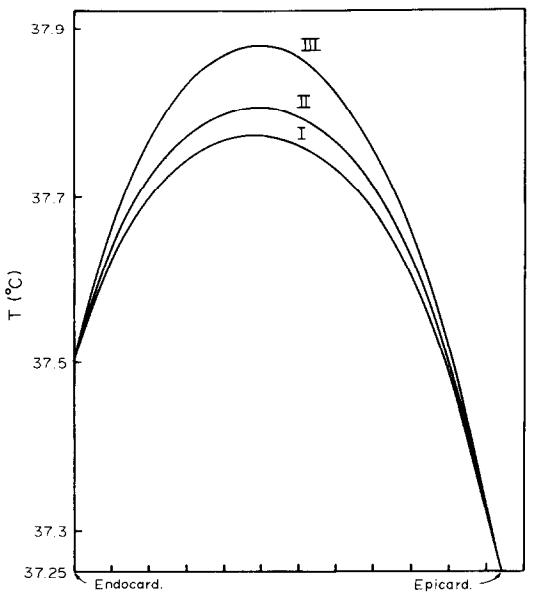

FIG. 7. The myocardial temperature distribution at $t = 0$, $T_b = 37.5°C$, $U_A = -0.25°C$, HR = 60 cpm. I, Normal perfusion rate; II, 0.8 × normal perfusion rate; III, 0.5 × normal perfusion rate.

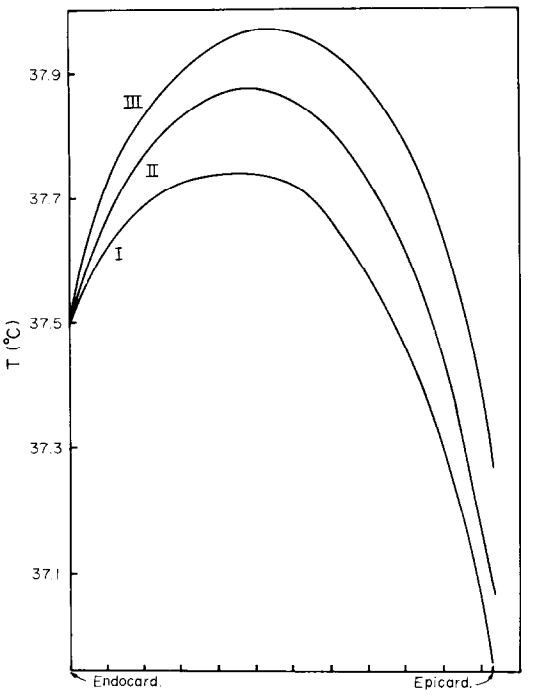

FIG. 9. The myocardial temperature distribution for $T_b = 37.5°C$, free convection at the epicardium with $h = 12.56$ W m^{-2} $°C^{-1}$. I, HR = 60 cpm; II, HR = 90 cpm; III, HR = 120 cpm.

The dependency of the epicardial temperature on the heart rate is shown in Fig. 9 for a specific value of h. As is to be expected, the higher the HR the higher the temperature at a point. An almost linear relation between h and the epicardial temperature is demonstrated in Fig. 10 for the different heart beats. Clearly, the better the ventilation the higher the HTC and the lower the epicardial temperature. Figure 11 shows the dependence of the epicardial temperature on the blood perfusion rate. As seen in Fig. 11 there is an inverse, nonlinear relation between these two parameters, indicating that the application of the epicardial temperature for the evaluation of the myocardial perfusion is not trivial. In this case it is noted that the solution of equations (1), (6), (8) and (9) cannot be used with the solution of equation (11) to define an approximation as we did in equation (17). However, the 'average' solution, of equation (1) is very useful as an initial approximation.

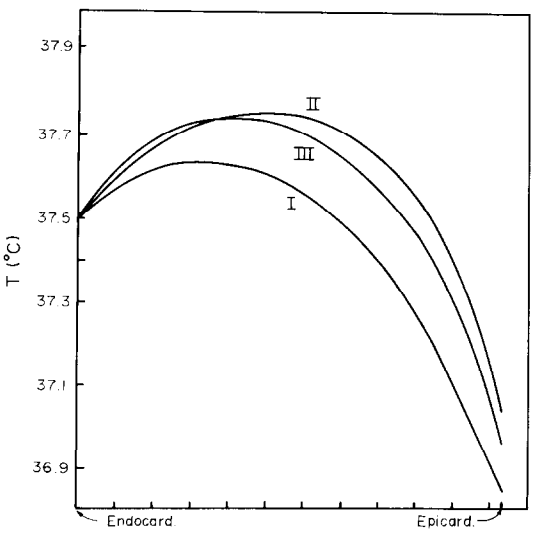

FIG. 8. The myocardial temperature distribution for $T_b = 37.5°C$, HR = 60 cpm, free convection at the epicardium with $h = 12.56$ W m^{-2} $°C^{-1}$. I, Time-independent solution using data of $t = 0$; II, 'average' solution, $\bar{u}$; III, complete time-dependent solution at $t = 0$.

6. COMPARISONS WITH EXPERIMENTAL DATA

A comparison of an actual instantaneous local myocardial temperature with our solution is difficult since measurements of instantaneous local perfusion are not currently available and the instantaneous local temperature cannot be reliably measured. However, a rough comparison with Ten Velden *et al.*'s [12] experimental data is possible. Ten Velden *et al.* [12] plotted the myocardial temperature distribution in the dog's LV and measured the blood perfusion in three sublayers of the LV muscle. In order to compare our analysis with the above measurements, the parameters of the human model (given in Table 2) were changed to correspond to the canine heart, and are given in Table 2. Utilizing a theoretical perfusion distribution which corresponds to the given experimental values within

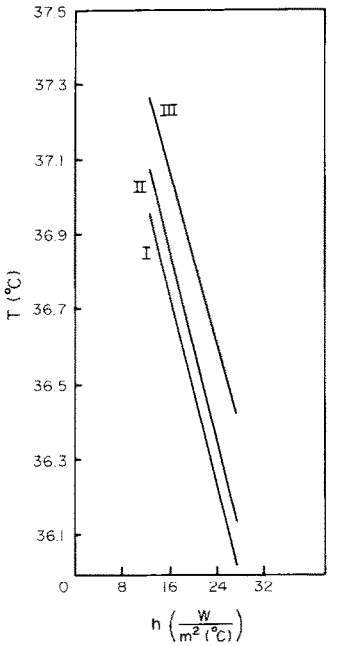

FIG. 10. The time epicardial temperature as a function of the free convection constant h. $T_b = 37.5°C$. I, HR = 60 cpm; II, HR = 90 cpm; III, HR = 120 cpm.

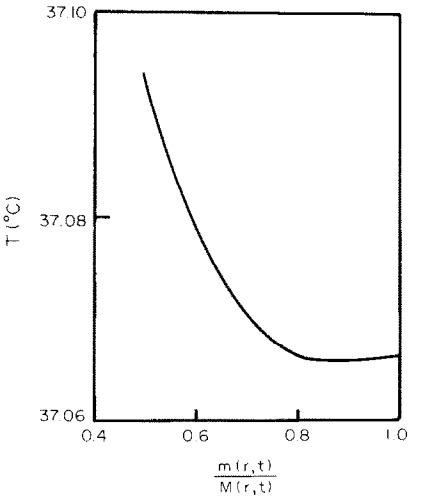

FIG. 11. The epicardial temperature as a function of the blood perfusion rate for $T_b = 37.5°C$, HR = 90 cpm, $h = 12.56$ W $m^{-2}\,°C^{-1}$. $\dot{M}(r,t)$ is the normal value of $\dot{m}(r,t)$ (see Table 2).

$\pm 15\%$, a comparison between the measured and the computed temperatures was done and shown in Fig. 12.

Although the agreement between the computed and experimental results is fair, the reported animal data is not sufficient for a reliable comparison, and the results show only a rough approximation. The differences between the experimental and theoretical curves may be attributed to a number of reasons: (a) differences in the actual (unknown) and calculated values of the oxygen consumption, as determined by the heart rate, blood pressure, preloading condition, basal metabolism etc.; (b) unsteady state and/or unstable conditions during the experimental measurements; (c) errors in the measurements; (d) errors in the parameter estimation by the model; and (e) errors induced by the symmetric simplification of the heat balance problem.

Also included in Fig. 12 is Ten Velden *et al.*'s analytical curves based on steady state and constant metabolic parameters. Evidently, this approximation is fair for certain conditions.

In order to get another indication as to the validity of our model, the veno-arterioral temperature difference ΔT_{VA}, that was reported by Neill *et al.* [15] is compared with the expected calculated difference which is given by

$$\Delta T_{VA} = \frac{\sum_{i=1}^{10} \frac{[T(r_i) + T(r_{i+1})]}{2} \cdot m[r_i, r_{i+1}] \cdot V[r_i, r_{i+1}]}{\sum_{i=1}^{10} m[r_i, r_{i+1}] \cdot V[r_i, r_{i+1}]} - T_b \qquad (18)$$

where $m[r_i, r_{i+1}]$ is the average blood volume that flows between r_i and r_{i+1} in one cycle and $V[r_i, r_{i+1}]$ is the (time averaged) volume of the muscle layer that extends from r_i to r_{i+1}.

Using equation (18) with $T_b = 37.5°C$, $u_A = 0.25°C$, 60 cpm $\leqslant$ HR $\leqslant$ 120 cpm, yields $0.003°C \leqslant \Delta T_{VA} \leqslant 0.288°C$ for the human model while Neill *et al.* [15] reported $0.14°C \leqslant \Delta T_{VA} \leqslant 0.32°C$ for dogs. Since the heart rates in dogs are usually higher (90–150 cpm) than those for humans, the resemblance is quite good.

7. DISCUSSION AND CONCLUSIONS

The instantaneous local temperature within the myocardium was evaluated here, based on the calculated coronary blood flow distribution and the local oxygen consumption. Two types of boundary conditions were used, corresponding to the closed chest heart and the open chest heart. Obviously, the latter situation allows for some arbitrary manipulation (say, cooling the epicardium) whereas in the former case the epicardial temperature is usually uncontrollable.

The main conclusions about the physiological processes related to the heat balance within the myocardium are:

1. The energy balance within the myocardium must account for the internal heat conduction, heat convection, and metabolic heat production, see Table 3.

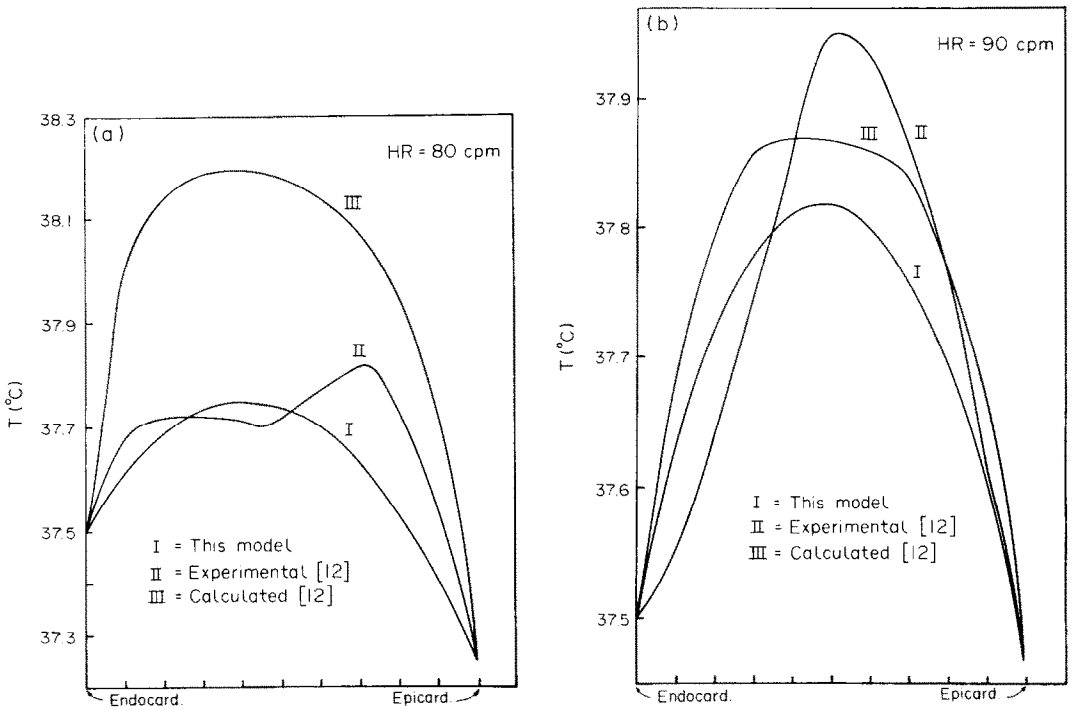

FIG. 12. Comparison of the computed canine myocardial temperature distribution with Ten Velden *et al.* [12] experimental and computed results. I, our solution; II, experimental data from [12]; III, computed results from [12]. A, HR = 80 cpm. B, HR = 90 cpm.

2. Increasing the heart rate and/or decreasing the blood perfusion causes a considerable increase in the myocardial temperature.

3. The myocardial temperature at any given point in space does not change, in any significant sense, during the contraction and relaxation phases of the heart's cycle and thus can be approximated reasonably well by the proposed, simplified, 'average' solution.

4. In the case of a closed chest heart, the temperature usually attains its maximum value at the mid-layer of the myocardium and the gradients of the temperature increase toward the internal and external boundaries (epicardium and endocardium).

5. In normal resting conditions of human heart, when the epicardial–endocardial temperature difference equals 0.25°C, the difference between the maximum and minimum temperatures within the wall is 0.6°C. For dog heart (working under rest conditions) the difference between the maximum temperature observed in the LV myocardium and the temperature in the ventricular cavity was found to be about 0.3°C. This result agrees with the measurements of Reynolds *et al.* [1] who found that this difference ranges between 0.06 to 0.70°C.

6. In the case of an open chest heart, an (almost) linear relation exists between the value of the free convection HTC (which reflects the effects of the environment of the heart) and the epicardial temperature.

7. As the epicardial temperature changes inversely with the perfusion ratio, this temperature may be used as a rough estimate of the coronary perfusion under steady state experimental conditions [11, 23]. The model approach suggested here may help in the estimation of the coronary perfusion from the epicardial temperature. Measuring the open chest

Table 3. Heat generation and transfer due to different mechanism in the myocardium. Data are for: HR = 90 cpm, T_b = 37.5°C, U_A = 0.25°C

Layer	Values of heat due to: Metabolic energy	Convection (diffusional heat)	Conduction
Subendocardium	0.033 J cm^{-3}	0.011 J cm^{-3}	0.023 J cm^{-3}
Subepicardium	0.026 J cm^{-3}	0.00044 J cm^{-3}	0.020 J cm^{-3}

epicardial temperature is sufficient for the computation of the temperature within the entire muscle.

To the best of our knowledge this is the first time that the instantaneous local temperature in the myocardium has been computed by using distributed blood perfusion and oxygen consumption data. Comparison of the analysis presented here with the few experimental data that are given in the literature gives a qualitative confirmation of the model. More accurate comparisons require more detailed data. The model's parameters are sure to help in establishing the kind of data taken and reported.

Acknowledgement—This study was supported by the Michael Kennedy-Leigh Fund, London, and sponsored by the MEP Group, Women's Division, American Technion Society, U.S.A. The cooperation of Prof. N. Westerhof in providing the experimental data is highly appreciated.

REFERENCES

1. E. W. Reynolds, Jr. and P. N. Yu, Transmyocardial temperature gradient in dog and men, *Circulation Res.* **15,** 11–19 (1964).
2. M. Weiss and W. Forrester, A model for the assessment of left ventricular compliance: the effect of hypertropy and infarction, *Cardiovas. Res.* **9,** 544–553 (1975).
3. A. L. Yettram, C. A. Vinson and G. D. Gibson, Computer modeling of the human left ventricle, *Trans. ASME* **104,** 148–152 (1982).
4. J. H. J. M. van der Broek and M. H. L. M. van der Broek, Application of an ellipsoidal heart model in studying left ventricular contractions, *J. Biomech.* **13,** 493–503 (1979).
5. A. F. Huxley, Energetics of muscle, *Chem. Brit.* **6,** 477–479 (1970).
6. A. M. Katz, Biochemical basis of cardiac contraction, in *Cardiac Mechanics* (edited by I. Mirsky, D. N. Ghista and S. Harold), pp. 67–86. J. Wiley, New York (1974).
7. W. W. Parmley and J. V. Tyberg, Determination of myocardial oxygen demand, *Prog. Cardiol.* **5,** 19–36 (1976).
8. R. J. Gordon, A general mathematical model of coronary circulation, *Am. J. Physiol.* **226,** 608–615 (1974).
9. R. B. Panerai, J. H. Chamberlain and B. Sayers, Characterization of the extravascular component of coronary resistance by instantaneous pressure–flow relationships in the dog, *Circulation Res.* **45,** 378–390 (1979).
10. E. O. Feigl, Coronary physiology, *Physiol. Rev.* **63,** 31–39 (1983).
11. E. J. Hernandez, J. K. Hoffman, M. Fabian, J. H. Siegeel and R. C. Eberhart, Thermal quantification of regional myocardial perfusion and heat generation, *Am. J. Physiol.* **236,** 345–355 (1979).
12. G. H. M. Ten Velden, G. Elzinga and N. Westerhof, Left ventricular energetics: heat loss and temperature distribution of canine myocardium, *Circulation Res.* **50,** 63–73 (1982).
13. B. H. Smaill, J. Douglas, P. J. Hunter and I. Anderson, Heat transfer in the left ventricle, in *Heat Perfusion, Energetics and Ischemia* (edited by L. Dintenfaas, D. G. Julian and G. V. E. Seaman), NATO ASI Series, Vol. 62, pp. 623–648 (1983).
14. R. C. Eberhart, Private communication (1984).
15. W. A. Neill, N. Krasnow, H. J. Levine and R. Gorli, Myocardial anaerobic metabolism in intact dogs, *Am. J. Physiol.* **204,** 427–432 (1963).
16. R. Beyar and S. Sideman, Time dependent coronary blood flow distribution within the left ventricular wall, Technion Res. and Dev. Report, No. 110 (1984).
17. R. Beyar and S. Sideman, Spatial energy balance within a structural model of the left ventricle, Technion Res. and Dev. Report, No. 111 (1984).
18. R. Beyar and S. Sideman, Computer study of the left ventricular performance based on its fiber structure, sarcomere dynamics and electrical activation propagation, *Circulation Res.* **55,** 358–374 (1984).
19. W. B. Keller, *Numerical Methods for Two Point Boundary Value Problems.* Ginn-Blasidell, Waltham, Massachusetts (1968).
20. C. L. Gibbs, Cardiac energetics, *Physiol. Rev.* **58,** 174–254 (1978).
21. W. A. Neill, H. J. Levine, R. J. Wagman, J. V. Messer, N. Krasnow and R. Gorlin, Left ventricular heat production measure by coronary flow and temperature gradient, *J. appl. Physiol.* **16,** 883–890 (1961).
22. J. P. Holman, *Heat Transfer*, p. 13. McGraw-Hill, Kogakusha (1976).
23. A. Shitzer and R. C. Eberhart, Estimation of tissue blood perfusion rate from diffusible indicator measurements: A sensitivity analysis, New York: American Society of Mechanical Engineers (79-WA/HT-73) (1979).
24. A. R. Mitchell and D. F. Griffiths, *The Finite Difference Method in Partial Differential Equations.* John Wiley, New York (1980).

APPENDIX A: PROOF OF STABILITY OF EQUATION (13)

1. *Closed chest solution*
Define

$$U_j^n = u_j^n - u\left(n0.01,\ r_0^n + \sum_{m=1}^{j-1} \Delta r_m^n\right) \tag{A1}$$

and express U_j^n as

$$U_j^n = \left(\prod_{k=1}^{n} \zeta_k\right) \exp\left[i\left(r_0^n + \sum_{m=1}^{j-1} \Delta r_m^n\right)\beta\right] \tag{A2}$$

where $\exp\left[i\left(r_0^1 + \sum_{m=1}^{i-1} \Delta r_m^1\right)\beta\right]$ is the initial error.

Then by the Von Neumann method [24] a sufficient condition for stability is $|\zeta_k| < 1$. Substitution of equation (A2) in equation (13) yields

$$\zeta_n = 1 + \alpha\Delta t\left\{c_1 + \frac{\Delta r_{j-1}^n e^{i\beta\Delta r_j^n} + \Delta r_j^n e^{-i\beta\Delta r_{j-1}^n} - (\Delta r_j^n + \Delta r_{j-1}^n)}{\frac{1}{2}\Delta r_j^n \Delta r_{j-1}^n (\Delta r_j^n + \Delta r_{j-1}^n)} + \frac{e^{i\beta\Delta r_j^n} - e^{-i\beta\Delta r_{j-1}}}{(\Delta r_j^n + \Delta r_{j-1}^n)\left(r_0^n + \sum_{m=1}^{j-1} \Delta r_m^n\right)}\right\}. \tag{A3}$$

The stability criterion is verified by substitution of Δr_j^n, $1/\alpha$, c_2, Δt in (A3).

2. *Open chest case*
Equation (13) is written in a matrix from as

$$\mathbf{U}^{n+1} = A^n \mathbf{U}^n + \mathbf{b}^n \tag{A4}$$

where A^n is a tridiagonal 10×10 matrix. Stability is assured if all the eigenvalues of A^n, $\lambda_i(A^n)$, satisfy $\lambda_i(A^n) < 1$. Writing A^n as a sum of two matrices

$$A^n = I + \alpha\Delta t\Omega^n \tag{A5}$$

where I is the identity $n \times n$ matrix, simplifies the proof. One can show, by evaluating the principal minors of $(-\Omega^n)$, that $(-\Omega^n)$ is a strictly positive definite matrix. This assures that the numerical solution actually converges to the analytic solution.

DISTRIBUTION DE TEMPERATURE DANS LA PAROI DU VENTRICULE GAUCHE DU COEUR

Résumé—La température instantanée locale T à la paroi du ventricule gauche est obtenue en résolvant l'équation du bilan d'énergie et en tenant compte de la création de chaleur instantanée dans la paroi musculaire. La demande de distribution d'oxygène et la perfusion locale coronarienne dépendant du temps, obtenues par un modèle mécaniste LV précédemment décrit, sont utilisées comme paramètres d'entrée dans l'équation de la chaleur. Des approximations du temps local moyen et des températures fonction du temps sont calculées pour deux types de conditions aux limites simulées expérimentalement : (a) coeur enfermé dans la poitrine et (b) couer dans la poitrine ouverte (exposé à l'air avec convection naturelle). Les effets sur T de la vitesse du coeur et la perfusion locale sanguine sont étudiés. La température locale est trouvée pratiquement inchangée pendant un cycle, avec des changements qui sont typiquement inférieurs à 0,005°C pendant un cycle. Néanmoins la température varie avec la position dans le myocarde et elle atteint son maximum au milieu des couches. Pour un coeur dans la poitrine fermée, on trouve une approximation de la température instantanée basée sur une solution 'moyenne'. Dans le cas d'un coeur dans une poitrine ouverte, on montre comment T dans le péricarde peut définir la distribution de température à travers toute la paroi musculaire. Les résultats calculés sont trouvés en bon agrément avec des études expérimentales sur des chienes.

TEMPERATURVERTEILUNG IM INNERN DER LINKEN HERZKAMMERWAND

Zusammenfassung—Die augenblickliche örtliche Temperatur T in der gesamten linken Herzkammerwand erhält man durch Lösen der Energiebilanzgleichung, die der augenblicklichen räumlichen Wärmeerzeugung in der Muskelwand Rechnung trägt. Sowohl der verteilte Sauerstoffbedarf als auch die zeitabhängige örtliche Herzkranzdurchblutung, welche auf dem früher beschriebenen mechanischen Modell der linken Herzkammer beruht, werden als Eingabeparameter für die Wärmebilanz verwendet. Näherungen der örtlichen Zeitmittelwerte und die zeitabhängigen Temperaturen werden für zwei Arten von experimentellen Randbedingungen berechnet: Simulation (a) bei geschlossenem Brustkorb (gegebene epikardiale Temperatur T) und (b) bei offenem Brustkorb (der Luft bei freier Konvektion ausgesetzt). Die Auswirkungen der Herzfrequenz und der örtlichen Durchblutungsmenge auf die Temperatur T wurden untersucht. Die örtliche Temperatur war praktisch unverändert während einer Periode, mit Schwankungen, die üblicherweise kleiner als 0,005 K während einer Periode sind. Die Temperatur verändert sich im Inneren des Myokardiums von Ort zu Ort und erreicht ihren Maximalwert in den mittleren Schichten. Bei geschlossenem Brustkorb wurden Näherungswerte für die augenblickliche Temperatur, basierend auf der 'Durchschnittslösung' ermittelt. Im Falle des geöffneten Brustkorbes wird gezeigt, wie die Temperatur T im Epikardium durchaus die Temperaturverteilung in der gesamten Muskelwand bestimmen kann. Die berechneten Ergebnisse stimmen bei ausreichender Genauigkeit mit experimentellen Untersuchungen an Hunden überein.

РАСПРЕДЕЛЕНИЕ ТЕМПЕРАТУРЫ ВНУТРИ СТЕНКИ ЛЕВОГО ЖЕЛУДОЧКА СЕРДЦА

Аннотация—Из решения уравнения баланса энергии, учитывающего мгновенное тепловыделение внутри мускульной стенки, получены значения температур T в стенке левого желудочка (LV). Исходными параметрами задачи теплопроводности являются как потребление кислорода, так и зависящая от времени локальная коронарная проницаемость, основанные на ранее описанной механической модели LV. Аппроксимации осредненных по времени локальных температур получены для двух типов экспериментальных граничных условий, моделирующих (а) сердце в закрытой грудной клетке (задана эпикардиальная T) и (б) сердце в открытой грудной клетке (подвержено действию воздуха со свободной конвекцией). Исследовано влияние ритма сердца и скорости локальной проницаемости крови на величины T. Локальная температура оказалась практически постоянной в течение всего цикла—изменения не провосходят 0,005 С. Однако температура зависит от места измерения в миокарде и достигает максимума в средних слоях. Для сердца в закрытой грудной клетке получено приближение мгновенной температуры, основанное на 'осреднении'. В случае (б) показано, как T в эпикарде может определять распределение температуры во всей мускульной стенке. Результаты расчетов хорошо согласуются с данными опытов, проведенных на собаках.